MOLECULAR AND CELLULAR BIOLOGY, Mar. 2006, p. 1644–1653 Vol. 26, No. 5
0270-7306/06/$08.00+0 doi:10.1128/MCB.26.5.1644–1653.2006

Gadd34 Requirement for Normal Hemoglobin Synthesis

Andrew D. Patterson,[1,2]† M. Christine Hollander,[2]‡ Georgina F. Miller,[3] and Albert J. Fornace, Jr.[2]*

NIH-GWU Graduate Partnerships Program in Genetics,[1] Gene Response Section, Center for Cancer Research, NCI,[2] and Division of Veterinary Resources, NIH,[3] Bethesda, Maryland

Received 15 December 2004/Returned for modification 21 January 2005/Accepted 8 December 2005

The protein encoded by growth arrest and DNA damage-inducible transcript 34 (Gadd34) is associated with translation initiation regulation following certain stress responses. Through interaction with the protein phosphatase 1 catalytic subunit (PP1c), Gadd34 recruits PP1c for the removal of an inhibitory phosphate group on the α subunit of elongation initiation factor 2, thereby reversing the shutoff of protein synthesis initiated by stress-inducible kinases. In the absence of stress, the physiologic consequences of Gadd34 function are not known. Initial analysis of *Gadd34*-null mice revealed several significant findings, including hypersplenism, decreased erythrocyte volume, increased numbers of circulating erythrocytes, and decreased hemoglobin content, resembling some thalassemia syndromes. Biochemical analysis of the hemoglobin-producing reticulocyte (an erythrocyte precursor) revealed that the decreased hemoglobin content in the *Gadd34*-null erythrocyte is due to the reduced initiation of the globin translation machinery. We propose that an equilibrium state exists between Gadd34/PP1c and the opposing heme-regulated inhibitor kinase during hemoglobin synthesis in the reticulocyte.

Thalassemia is a relatively common single-gene disorder, with roughly 90% of patients having defective hemoglobin associated with mutations in the globin genes (8). Of those remaining patients having normal α- and β-globin genes, some evidence suggests that improper regulation and expression of globin genes may represent another molecular explanation for this disease. For example, patients with X-linked α-thalassemia/mental retardation syndrome exhibit α-thalassemia resulting from the mutation of a general transcription factor needed for α-globin expression (7). Another novel molecular explanation may in fact lie within aberrant or deregulated translation of otherwise normal globin chains. Moreover, improper regulation of translation initiation may represent one explanation for decreased synthesis of globin proteins in patients without any known globin gene mutations.

Translation initiation involves the concerted efforts of several proteins whose functions are to assemble the ribosomal subunits and mRNA. The three-subunit (α, β, and γ) translation initiation factor eIF2 represents a key component in translation initiation regulation (23). Its function involves the recruitment of new initiator Met-tRNAs to form the 43S preinitiation complex (22). Stress responses initiated by several kinases, including GCN-2 kinase, heme-regulated inhibitor (HRI) kinase, PERK, and PKR are associated with the phosphorylation of eIF2α on serine 51 [p-eIF2αS51)] (9–11, 33). In the phosphorylated form, eIF2α remains tightly complexed with GDP and the guanine nucleotide exchange factor eIF2B, thereby preventing exchange of GDP for GTP, which prevents new rounds of translation initiation (14). The inhibitory state of p-eIF2α(S51) can be reversed by the protein encoded by *Ppp1r15a* (herein referred to as *Gadd34*) when it recruits the protein phosphatase 1 catalytic subunit (PP1c) to dephosphorylate p-eIF2α(S51) (3, 6, 19).

During endoplasmic reticulum (ER) stress, the induction of growth arrest and DNA damage-inducible transcript 34 (Gadd34) represents a negative feedback loop of the stress response during the transient inhibition of translation (13, 18–20). During the stress response and subsequent translation repression, activating transcription factor 4 (ATF4) is induced due to unmasking of its true open reading frame (29). It can then bind the promoter of *Gadd34*, which leads to its induction and subsequent reversal of the stress response (18, 19). In addition, it appears that Gadd34 protein induction reinforces the expression of ATF4 for the attenuation of the stress response (13, 20). Several groups have reported that in the absence of Gadd34, recovery from the PERK-modulated ER stress response is severely delayed, demonstrating the crucial role for Gadd34 in timely ER stress response attenuation (13, 20).

However, while Gadd34 has a clear role in the ER stress response, and given that eIF2α(S51) is a target of at least three other kinases (GCN-2, HRI, and PKR), it is possible that Gadd34 may function in contexts outside of the ER stress response. For example, GCN-2 kinase is activated during amino acid deprivation and phosphorylates eIF2α(S51) to attenuate translation initiation (33). Like the stress response attenuation following PERK signaling, it has been speculated that Gadd34 induction may be responsible for the attenuation of GCN-2 kinase signaling (i.e., another Gadd34 negative feedback loop) (19). The importance of Gadd34 expression is highlighted by findings showing that failure to reverse translation inhibition (e.g., in the *Gadd34*-null mouse) may result in apoptosis due to sustained levels of p-eIF2α(S51) (28). In fact, *Gadd34*-null cells were more sensitive to thapsigargin treatment, suggesting that sustained levels of p-eIF2α(S51) may be an adverse consequence of Gadd34 loss (20).

* Corresponding author. Mailing address: Department of Genetics and Complex Diseases, Harvard School of Public Health, Boston, MA 02115. Phone: (617) 432-5892. Fax: (617) 432-5236. E-mail: afornace@hsph.harvard.edu.

† Present address: Molecular Biology of Selenium Section, Laboratory of Cancer Prevention, Center for Cancer Research, National Cancer Institute, National Institutes of Health, Bethesda, MD 20892.

‡ Present address: Cancer Therapeutics Branch, Center for Cancer Research, National Cancer Institute, National Institutes of Health, Bethesda, MD 20889.

Gadd34 was also discovered as a transcript (Myd116) increased in terminally differentiating myeloid cells (16). Therefore, another attractive context for Gadd34/PP1c activity might be to attenuate the cytoplasm-localized HRI kinase in reticulocytes that functions to prevent globin protein overproduction in the absence of heme (9, 16). When heme is abundant, HRI kinase activity is inhibited through the binding of two heme groups, and protein synthesis initiation proceeds with eIF2α(S51) unphosphorylated (4, 24). However, when heme quantities decline (e.g., due to iron deficiency), HRI becomes active through an autophosphorylation loop and phosphorylates eIF2α(S51) to inhibit the translation machinery so that globin production matches heme abundance (2, 25). In the absence of any apparent stress, *HRI*-null mice have mild hyperchromia and macrocytic erythrocytes (9). In a severe-stress environment (e.g., due to iron deficiency) the phenotype of *HRI*-null mice is profoundly exacerbated, and the failure to decrease translation of globin in reticulocytes results in the overproduction of globin proteins and subsequent hemolysis of erythrocytes (9). These observations suggest that HRI kinase modulates eIF2 activity both in a basal and in a stress-inducible fashion to alter globin translation.

Recent studies with *Gadd34*-null mice show that Gadd34 is necessary for recovery from the ER stress response, as mouse embryo fibroblasts (MEFs) from these mutant mice have delayed translation initiation recovery following treatments that interfere with protein synthesis and folding, such as thapsigargin and dithiothreitol treatment (13, 20). Interestingly, no observable phenotype for the *Gadd34*-null mice has been reported in the absence of stress, yet there is precedent that perturbation of eIF2 regulation can lead to an observable phenotype in the mouse (e.g., *PERK*-null mice are prone to early-onset diabetes, and *HRI*-null mice have hemoglobin synthesis abnormalities) (9, 10). It has been suggested that the loss of Gadd34 may have important effects on tissues such as pancreatic β cells, since β cells are undergoing high-throughput protein synthesis and proinsulin processing (20). Generally, those tissues requiring high rates of protein synthesis, such as β cells for insulin, B cells for antibodies, or reticulocytes for hemoglobin, could be affected by disruption of Gadd34 function.

In order to ascertain the function of Gadd34 in vivo, we generated *Gadd34*-null mice. Phenotypically, we found them to have a mild thalassemia-like condition, as characterized by erythrocytes with reduced hemoglobin content, smaller cell volume, and erythrocyte hyperplasia. Here we present evidence supporting a basal role for Gadd34 as a modulator of translation initiation with respect to globin translation and heme abundance. Moreover, we propose that an equilibrium state exists between Gadd34 and HRI during the synthesis of hemoglobin.

MATERIALS AND METHODS

***Gadd34* gene targeting, Southern blotting, PCR, and Northern blotting.** Mice were housed in Plexiglas cages and fed autoclaved NIH 31 diet and water ad libitum. The NIH is an AAALAC-accredited animal facility, and all studies were performed under an approved animal study protocol. The *Gadd34*-null mouse was generated by excising the coding regions (exons 2 and 3) of the mouse gene *Gadd34* using a Cre-LoxP approach (32). The *Gadd34*-null targeting vector containing the neomycin cassette and LoxP sites was electroporated into 129-derived ES cells and injected into C57BL/6 blastocysts. Mice containing the *Gadd34*-null targeted allele were crossed with mice expressing an eIIA-Cre recombinase transgene, generating *Gadd34*-null mice (15). *Gadd34*-null mice were backcrossed with a C57BL/6 mouse to remove the eIIA-Cre recombinase transgene. Southern blots of BamHI-digested genomic DNA were used to determine the wild-type (8.6-kb) and *Gadd34*-null (6.1-kb) alleles using a probe located 3′ from exon 3 of *Gadd34*. A multiplex PCR approach was used with primer pair Pr25 (5′-GCAGAGTTGGGTGTGAGCAATG-3′) and Pr26 (5′-AGGAGATAGAA GTTGTGGGCGTC-3′) (wild-type allele, 242 bp) and primer pair Pr25 and Pr54 (5′-TACTGGGATGACAAAGCACGC-3′) (*Gadd34*-null allele, 489 bp). For Northern blot analysis, mRNA was extracted from intestine, kidney, and spleen using a modified guanidine thiocyanate method (5). A full-length mouse *Gadd34* cDNA was used to detect the expression of *Gadd34*, and a full-length *Gapdh* probe was used for a loading control. Radioactive blots were exposed to a phosphorimager cassette and imaged using a Storm scanner (Amersham).

Pathology. Several 4-month-old wild-type, heterozygous, and *Gadd34*-null mice from each sex were phenotyped by a board-certified veterinary pathologist. Complete blood counts (CBCs) were performed using the Hemavet HV950FS (Drew Scientific), and peripheral blood smears were made using the DiffSpin2 Slide Spinner (Statspin, Inc.) in order to better preserve the morphology of the blood cells (31). Peripheral blood smears were dried and stained according to the manufacturer's instructions (Hematology 3 Step Stain; Richard Allen Scientific). Spleens were embedded in paraffin, sectioned, and stained with hematoxylin and eosin (HE).

Erythrocyte precursor assay. Spleens from six age-matched wild-type and *Gadd34*-null mice were prepared as described previously (27). Cells were washed twice in phosphate-buffered saline (PBS) containing 0.5% bovine serum albumin (BSA). One million cells were resuspended in 0.5% BSA–PBS and incubated with phycoerythrin-conjugated anti-mouse CD71 (1 μg) (C2; BD Pharmingen) and APC-conjugated rat anti-mouse Ter119 (1 μg) (Ly-76; BD Pharmingen) for 20 minutes at room temperature. The cells were washed once with 0.5% BSA–PBS and resuspended in 500 μl of PBS containing 7-amino-actinomycin D (1:1,000) (BD Pharmingen). Viable cells staining positively for Ter119 were gated and used for analysis. Samples were analyzed by FACSCalibur (BD Biosciences) and the CellQuest software package (BD Biosciences). Mature erythroid precursors were calculated by first determining the $CD71^{hi}$ and $CD71^{lo}$ fractions. The $CD71^{lo}$ fraction was then divided by the sum of $CD71^{hi}$ and $CD71^{lo}$ to yield the percentage of mature erythroid cells.

Erythrocyte half-life determination. A group of five age-matched males and females from each genotype was injected intraperitoneally with *N*-hydroxysuccinimido (NHS)–biotin (Sigma) on days −2 and −1 at 150 mg/kg of body weight. On day zero and then every fourth or fifth day, 5 μl of tail tip blood was collected in 1 ml of PBS. The blood samples were spun at 1,000 × *g* for 10 min, resuspended in PBS containing 1 μg of fluorescein isothiocyanate-streptavidin, and incubated for 10 min at room temperature in the dark. The samples were spun at 1,000 × *g* for 10 min and resuspended in 500 μl of PBS. Fluorescence-activated cell sorter (FACS) analysis of samples was performed by FACSCalibur and analyzed with CellQuest software. The value at day zero was considered 100% (90 to 95% of the red cell population was actually labeled for each sample), and subsequent samples were normalized to this time point.

Erythrocyte osmotic fragility. Blood was obtained from three 2- to 4-month-old wild-type and *Gadd34*-null mice from the mandibular artery and diluted 1:10,000 in PBS for cell counting. Ten million erythrocytes were placed in solutions containing either 0.9% (physiologic saline) NaCl or in a hypotonic solution containing 0.85, 0.68, 0.61, 0.59, 0.56, 0.53, 0.47, 0.42, 0.30, or 0.0% NaCl. Samples were mixed and incubated for 10 minutes and then briefly spun for 1 minute at 16,000 × *g* to pellet intact erythrocytes. The supernatant was analyzed for released hemoglobin from lysed cells by measuring the absorbance of hemoglobin at 540 nm. Samples were normalized to complete lysis (0% NaCl) for each mouse. *P* values were calculated by analysis of variance (ANOVA).

Hemoglobin electrophoresis. Blood (50 to 100 μl) obtained from three wild-type and *Gadd34*-null mice was washed two times with PBS and lysed in four packed cell volumes of deionized water. The samples were spun at 10,000 × *g* for 10 minutes to remove any insoluble material. Twenty microliters of the hemoglobin lysate was incubated in 1 milliliter of Drabkin's reagent (Sigma) for 20 minutes. The sample absorbance was read at 540 nm, and the hemoglobin concentration was calculated. Twenty-five micrograms of hemoglobin was mixed with loading buffer (6 M urea, 10% glacial acetic acid, 10% β-mercaptoethanol, and 0.03% pyronin Y) and separated on a Triton-acid-urea (TAU) gel (12.5% polyacrylamide, 4 M urea, 5% glacial acetic acid, 2% Triton X-100) as described previously (1). The gel was fixed in a solution containing 10% methanol, 10% glacial acetic acid, and 0.5% Coomassie blue R-250 and destained by diffusion in a solution containing 10% methanol and 10% glacial acetic acid. The fixed gel was scanned on an Odyssey Infrared Imaging System (Li-Cor Biosciences) in order to quantitate the expression of globin chains.

Reticulocyte enrichment. Mice were injected intraperitoneally with 40 mg/kg of body weight of phenylhydrazine dissolved in sterile PBS on days zero, one, and three as described previously (9). Reticulocyte enrichment was monitored by FACS using 1 microliter of blood from the tail tip diluted in 1 milliliter of ReticCount Reagent (BD Biosciences). When reticulocyte levels reached greater than 85% of the total blood cell population (6 to 7 days after first injection), the mice were anesthetized and blood was collected by cardiac puncture. The blood was placed immediately in ice-cold PBS supplemented with 5 mM glucose and washed twice.

Cell culture, Western analyses, and protein synthesis assays. MEFs were generated by crossing *Gadd34*-heterozygous mice, and embryos were harvested at embryonic day 12.5. The MEFs were seeded at 2×10^5 cells/ml and 2 days later treated with 1 μM thapsigargin for Gadd34 induction for 1, 3, 5, and 7 hours. The cells were lysed in 20 mM HEPES (pH 7.5), 1% Triton X-100, 150 mM NaCl, 10% glycerol, 1 mM EDTA, and protease inhibitors (Complete Mini Protease Inhibitor Cocktail; Roche Diagnostics). Normalized protein lysates (BCA Protein Assay Kit; Pierce) were separated on 12% sodium dodecyl sulfate-polyacrylamide gels, transferred to polyvinylidene difluoride membranes, and stained with antibodies detecting Gadd34 (1:200) (C-19; Santa Cruz Biotechnology, Inc.) or actin (1:10,000) (Ab-1; Oncogene Research Products).

For eIF2α(S51) phosphorylation status in mouse reticulocytes, cells were seeded at 1×10^8 cells/ml in Dulbecco modified Eagle medium supplemented with dialyzed 2% fetal bovine serum and 2 mM glutamine as described previously (9). The reticulocytes were allowed to recover for 1 hour at 37°C and stimulated with 40 μM hemin (Sigma). Aliquots (100 μl) were taken before hemin addition (time zero) and then at 30 min and 1, 2, and 3 h after hemin addition. The reticulocyte protein lysates were separated on 12% sodium dodecyl sulfate-polyacrylamide gels, transferred to polyvinylidene difluoride membranes, and stained with antibodies as described above or with p-eIF2α(S51) (1:1,000) [p-eIF2α(S51); Cell Signaling Technology] and total eIF2α (1:1,000) (Fl-315; Santa Cruz Biotechnology, Inc.). Densitometry measurements were performed using ImageQuantTL and used to calculate p-eIF2α(S51)-to-total-eIF2α ratios.

For polysome analysis, approximately 150 μl of reticulocyte-enriched whole blood was immediately diluted in 1 ml of PBS supplemented with 100 μg/ml cycloheximide (PBS/CHX). The reticulocytes were washed two more times with PBS/CHX and lysed in buffer containing 20 mM Tris-HCl (pH 7.5), 20 mM $MgCl_2$, 60 mM NaCl, 10 mM $MgCl_2$, 1 mg/ml heparin, 1% Triton X-100, and 100 μg/ml CHX. The lysate was cleared in a microcentrifuge at 12,000 rpm for 15 min at 4°C, and the supernatant was frozen on dry ice. Sixteen optical-density-at-260-nm (OD_{260}) units of the supernatant were layered on a continuous 4 to 47% sucrose gradient containing 10 mM $MgCl_2$ and 1 mM dithiothreitol. The gradients were centrifuged in an SW41 rotor at 4°C at 39,000 × *g* for 2.5 h. The gradients were analyzed at 254 nm using an ISCO UA-6 detector, and the polysome-to-monosome ratios were calculated by determining the area under the monosome and polysome peaks.

Iron-deficient diet. Weanling wild-type (basal diet, five males and two females; iron-deficient diet, six males and three females) and *Gadd34*-null (basal diet, three males and three females; iron-deficient diet, four males and four females) mice were placed either on an iron-deficient diet (Purina Test Diet, Low Iron PD 5859) or on a control basal diet (Purina Test Diet, Basal 5755). The residual iron in the iron-deficient diet was reported to be 10 to 20 ppm. Food and autoclaved, distilled, deionized water were given ad libitum. After 2 weeks on the diets, exactly 50 μl of blood was obtained from the retroorbital cavity and placed in a tube containing EDTA and 150 μl of PBS. CBCs were completed for each sample and adjusted based on the fourfold dilution. Blood was then collected every 2 weeks and analyzed as before. After 8 weeks on the iron-deficient diet, mice were returned to the basal diet. For the next 8 weeks, blood was collected every second week and analyzed as before. Samples were averaged for each genotype and plotted over time for each CBC parameter. Slopes for mean corpuscular volume (MCV) and mean corpuscular hemoglobin (MCH) were calculated from the best-fit line from week 8 to week 14 and averaged. *P* values were calculated by ANOVA.

RESULTS

Characterization of *Gadd34*-null mice. The mouse *Gadd34* gene consists of three exons, the last two of which encode the Gadd34 protein (Fig. 1A). The *Gadd34*-null targeted allele was generated by introducing a neomycin resistance cassette flanked by two LoxP sites (EcoRI) in the first intron, with a third LoxP site (AflIII) at the end of exon 3 (Fig. 1A, middle). *Gadd34*-null mice were generated by crossing the *Gadd34*-floxed mice with mice expressing an eIIa-Cre recombinase transgene, which is expressed during early embryogenesis (Fig. 1A, bottom) (32). Wild-type, heterozygous, and recombined *Gadd34*-null alleles were identified by genomic Southern blotting (Fig. 1B, top) and multiplex PCR (Fig. 1B, bottom).

To confirm the absence of *Gadd34* expression in the *Gadd34*-null mice, Northern blots of mRNA harvested from the intestine, kidney, and spleen were hybridized with full-length mouse *Gadd34* cDNA (Fig. 1C, top) and *Gapdh* cDNA (Fig. 1C, bottom). *Gadd34* is expressed in wild-type intestine, kidney, and spleen, while it is not expressed in *Gadd34*-null tissues.

Gadd34 protein induction was assessed by treating wild-type and *Gadd34*-null MEFs with thapsigargin, a potent Ca^{2+} ATPase inhibitor. After 3 hours, wild-type MEFs showed a robust increase in a roughly 100-kDa protein corresponding to the molecular mass of Gadd34 (Fig. 1D, left) (13, 20). However, as expected, the *Gadd34*-null MEFs showed no expression (Fig. 1D, right).

Pathological findings. After successful removal of the *Gadd34* coding regions and identification of the *Gadd34*-null mice, we sought to identify any physiologic abnormalities associated with Gadd34 loss. Initial phenotyping of the *Gadd34*-null mice revealed several hematologic abnormalities, implicating defects associated with cells of the erythrocyte lineage. *Gadd34*-null mice, irrespective of sex, have proportionally (spleen-to-brain ratio) larger spleens. Direct spleen weights confirmed this finding, with wild-type spleens averaging 0.075 g and *Gadd34*-null spleens averaging 0.115 g ($P = 0.0072$) (Fig. 2A). When scoring was done for erythroid precursor maturation using the general erythroid-specific marker Ter119 and the CD71 marker that is lost during maturation, FACS analysis of spleen cells demonstrated that the *Gadd34*-null mice have a significantly smaller percentage (92.3% in wild-type and 59.6% in *Gadd34*-null mice; $P < 0.0001$) of mature erythroid precursors in the spleen (Fig. 2B). *Gadd34*-null HE-stained spleens show an enrichment of nucleated, immature cells in the red pulp (Fig. 2C, right).

Further hematologic analysis, including CBC analyses, showed that the *Gadd34*-null mice have significant reductions in hemoglobin and mean corpuscular hemoglobin content, as well as a smaller mean corpuscular volume (Table 1). The *Gadd34*-null mice have a similar hematocrit resulting from the increased red blood cell numbers. The red blood cell distribution width demonstrates a wider range of erythrocyte size and shape in the *Gadd34*-null mice. Peripheral blood smears confirmed the CBC analysis, revealing that *Gadd34*-null mouse erythrocytes have weaker staining for hemoglobin (Fig. 3, bottom panel) than do their wild-type counterparts (Fig. 3, top panel). In addition, some *Gadd34*-null mouse erythrocytes are developmentally and morphologically abnormal, as demonstrated by the presence of target cells (darkly staining center surrounded by a pale area), Howell-Jolly bodies (nucleic acid remnants), and spiculocytes (erythrocytes with small, evenly spaced protrusions) (Fig. 3, bottom panel).

Erythrocyte fragility and half-life analysis. A simple and routine diagnostic test for hemoglobinopathies is determination of the osmotic fragility of red blood cells, in which thalassemic red blood cells will be more resistant to lysis in hypotonic solutions (30). Since erythrocyte hemolysis in hypotonic solu-

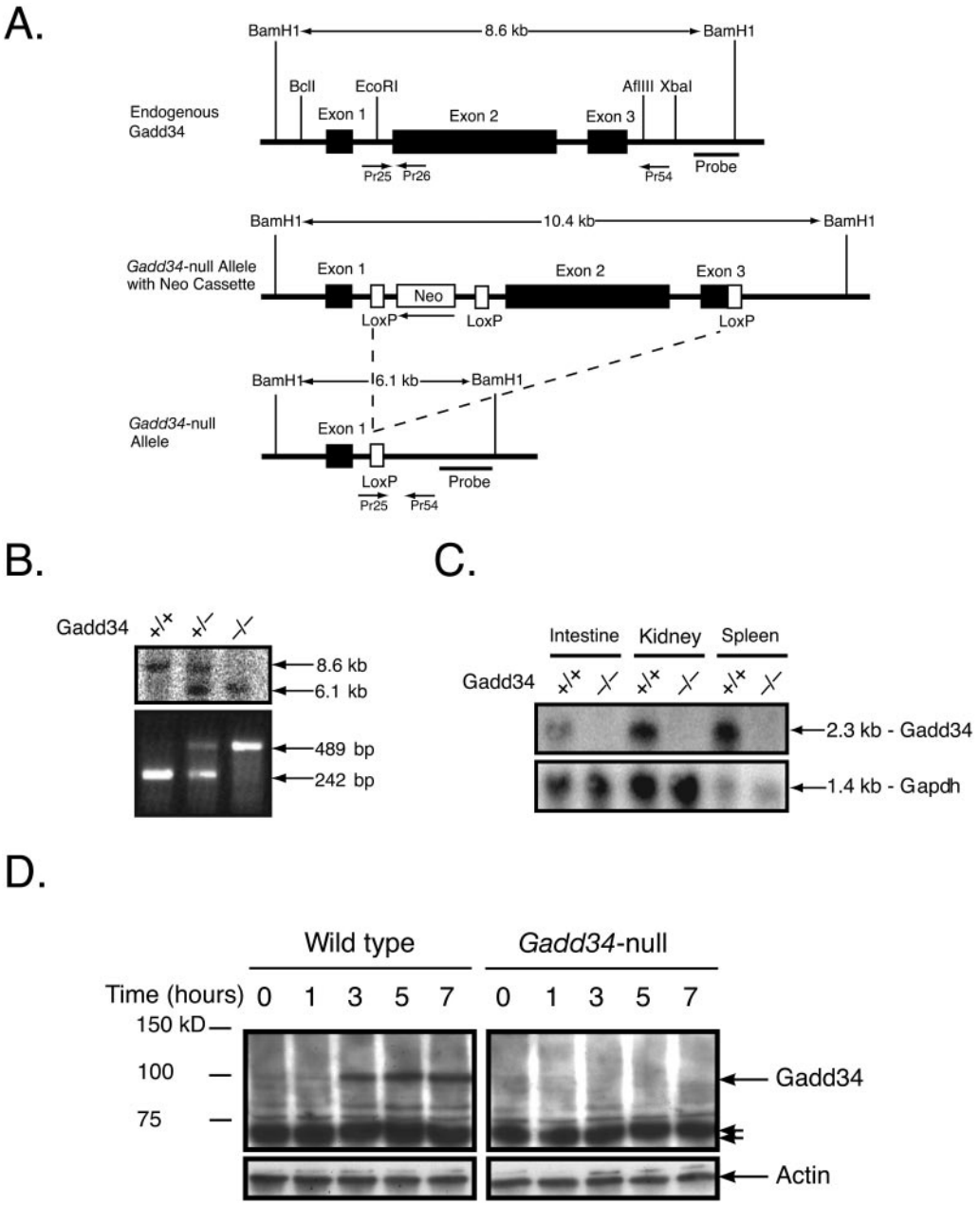

FIG. 1. Excision of the *Gadd34* coding region. (A) The *Gadd34* gene was excised from the mouse genome by flanking the second and third exons (black rectangles) with LoxP (white rectangles) recombination sites. Top, a schematic representation of the *Gadd34* gene in the mouse genome; middle, the *Gadd34*-null targeted allele containing the neomycin cassette and LoxP sites; bottom, the *Gadd34* coding region deleted allele after crossing *Gadd34*-null targeted mice with mice expressing an eIIa-Cre recombinase transgene. (B) After crossing with the Cre recombinase transgenic mice, *Gadd34*-null mice were identified by genomic Southern blotting using BamHI-digested genomic DNA (top); to facilitate high-throughput genotyping, a multiple PCR approach (bottom) was used to identify the wild-type (Pr25 and Pr26) and *Gadd34*-null (Pr25 and Pr54) alleles. (C) Absence of Gadd34 mRNA in *Gadd34*-null mice was confirmed by Northern blotting. mRNA from wild-type and *Gadd34*-null intestine, kidney, and spleen was probed using a full-length mouse *Gadd34* cDNA probe (top) and a *Gapdh* probe (bottom) as a loading control. (D) Wild-type and *Gadd34*-null early-passage embryonic day 12.5 MEFs treated with 1 μM thapsigargin and harvested at 0, 1, 3, 5, and 7 hours later. Wild-type MEFs show induction of Gadd34 by 3 hours posttreatment, with *Gadd34*-null MEFs showing no induction. Arrow doublets point to nonspecific bands. Actin is present as a loading control.

tions depends on the particular hemoglobin concentration, osmotic fragility plots can be generated to identify thalassemic blood samples (30). Similar to erythrocytes from thalassemia patients, *Gadd34*-null erythrocytes are more resistant to hemolysis in hypotonic solutions (Fig. 4A). Wild-type erythrocytes show greater than 50% hemolysis in a hypotonic solution containing 0.56% NaCl. However, in the 0.56% NaCl solution the *Gadd34*-null erythrocytes remained largely unaffected and showed no significant change in hemolysis levels above that observed in the physiologic ($P < 0.01$ [from 0.61% to 0.47%

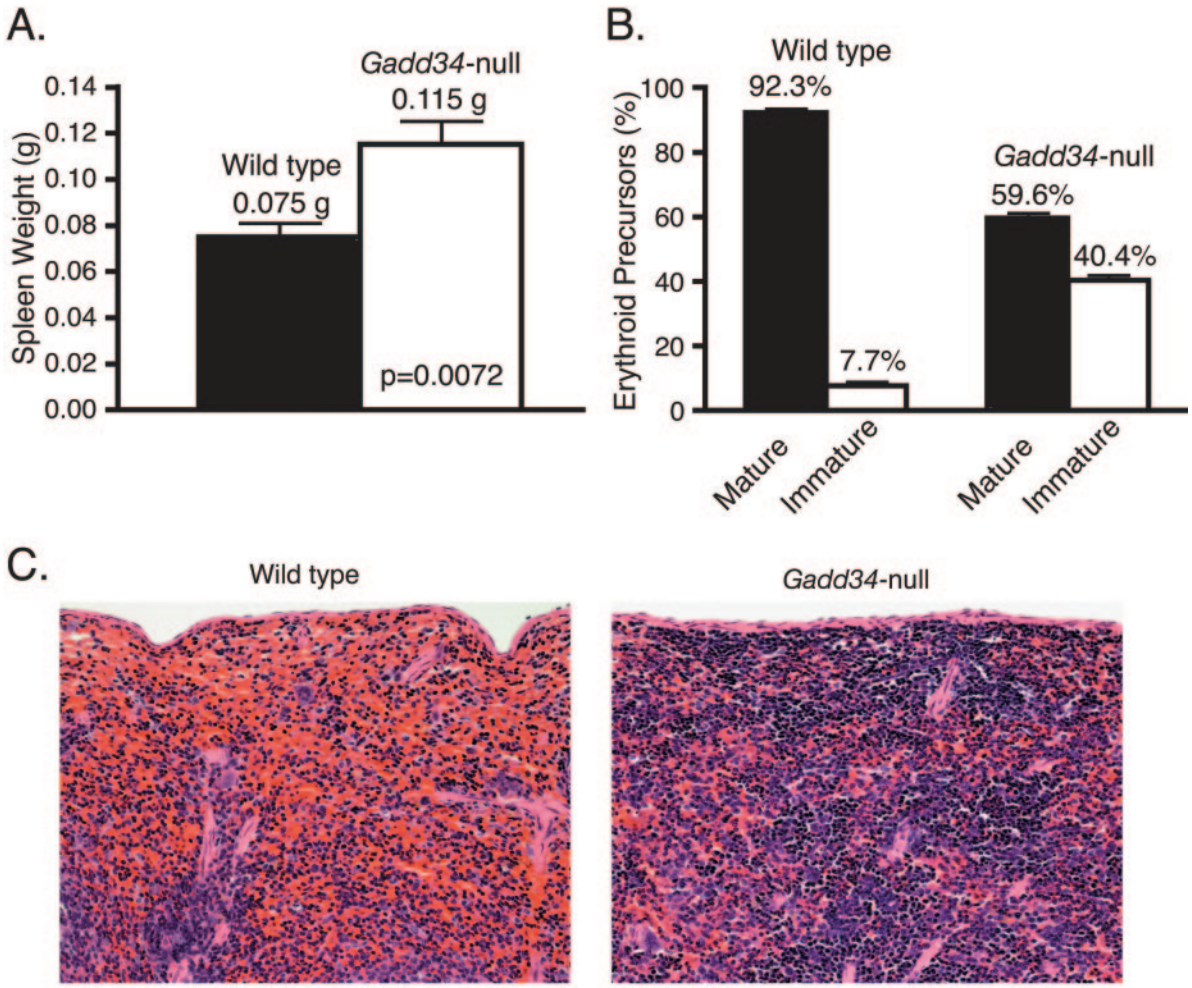

FIG. 2. *Gadd34*-null mice have hypersplenism and decreased numbers of mature erythroid precursors. (A) Direct spleen weights of 4-month-old wild-type and *Gadd34*-null mice. Data are plotted as means for six animals from each genotype ± standard errors of the mean (SEM) (P = 0.0072). (B) Average mature (black bars) and immature (white bars) erythroid precursors in the spleen calculated (mature = $CD71^{lo}$ divided by $CD71^{hi}$ + $CD71^{lo}$) for six animals from each genotype ± SEM. (C) *Gadd34*-null spleens have increased numbers of nucleated cells in the red pulp. Sections of spleen from wild-type (left) and *Gadd34*-null (right) mice were stained with HE. Magnification, ×20.

NaCl]), isotonic solution. Only in solutions of much weaker ionic strength do *Gadd34*-null erythrocytes begin to hemolyze (<0.47% NaCl), while at these concentrations the wild-type erythrocytes are completely hemolyzed.

Since *Gadd34*-null erythrocytes have abnormal morphology/physiology, and since the spleen is enlarged, we wished to understand how this state affected the half-life of the erythrocytes. By measuring the disappearance of NHS-biotin in the blood of both wild-type and *Gadd34*-null mice, a good estimate of the half-life of the erythrocytes was determined (Fig. 4B). The half-life of the wild-type erythrocytes was found to be approximately 17 days, while the *Gadd34*-null erythrocyte half-life was 21.6 days. However, the difference in half-life was not statistically significant (P = 0.19).

TABLE 1. Hematologic parameters of *Gadd34*-null mice

Parameter[a]	Mean value ± SEM for mice:		P^b
	Wild type (n = 8)	*Gadd34* null (n = 9)	
Hematocrit	41.9 ± 1.3	40.9 ± 0.9	NS
Hb (g/dl)	12.9 ± 0.3	11.0 ± 0.3	0.0004
RBC (10^6/μl)	8.7 ± 0.2	10.8 ± 0.3	<0.0001
MCHC (g/dl)	30.9 ± 1.0	28.9 ± 1.0	0.0013
MCV (fl)	47.8 ± 1.5	38.2 ± 1.0	<0.0001
RDW (%)	17.0 ± 0.2	23.7 ± 0.4	<0.0001

[a] Hb, hemoglobin. RBC, red blood cell. MCHC, mean corpuscular hemoglobin content. RDW, RBC distrubution width.
[b] P values were calculated with an unpaired t test. NS, not significant.

Hemoglobin synthesis. Since causes of thalassemia mostly include mutation of the globin genes, resulting in their under- or nonexpression, we sought to confirm that the hemoglobin chains were being synthesized appropriately in *Gadd34*-null mice. Wild-type and *Gadd34*-null mice express β_{major}-, β_{minor}-, and α-globin chains due to the genetic background of the parental mice (21). TAU gel electrophoresis of globin chains from both wild-type and *Gadd34*-null mice demonstrated that each genotype expresses all three forms of globin chains with no other globins (e.g., embryonic globins) being detected (Fig. 5). The ratios of α- and total β-globin generally did not differ

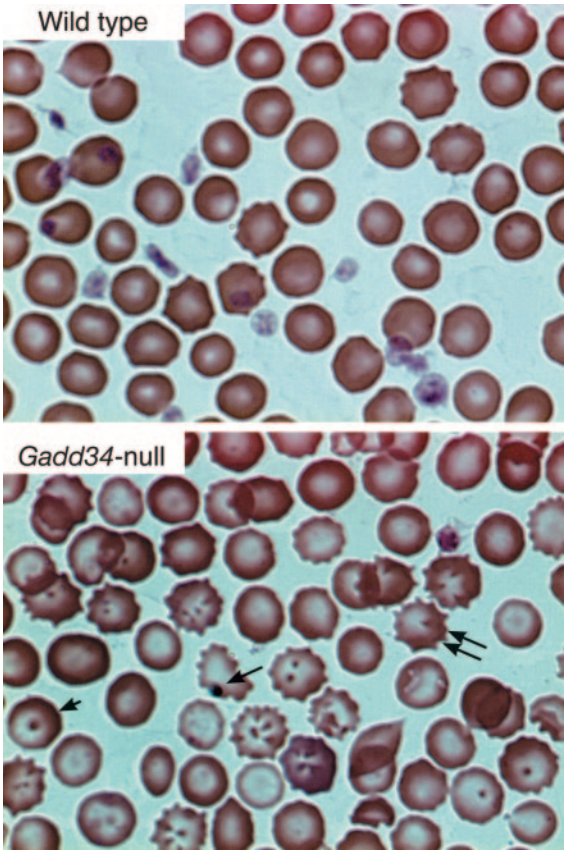

FIG. 3. *Gadd34*-null mice manifest erythrocyte abnormalities. Blood smears of erythrocytes from wild-type and *Gadd34*-null mice stained with eosin Y, azure A, and methylene blue under ×1,000 magnification. *Gadd34*-null mouse erythrocytes show weaker staining (decreased hemoglobin) and general erythrocyte morphological abnormalities. A target cell is marked by an arrowhead, a Howell-Jolly body by an arrow, and a spiculocyte by a double arrow.

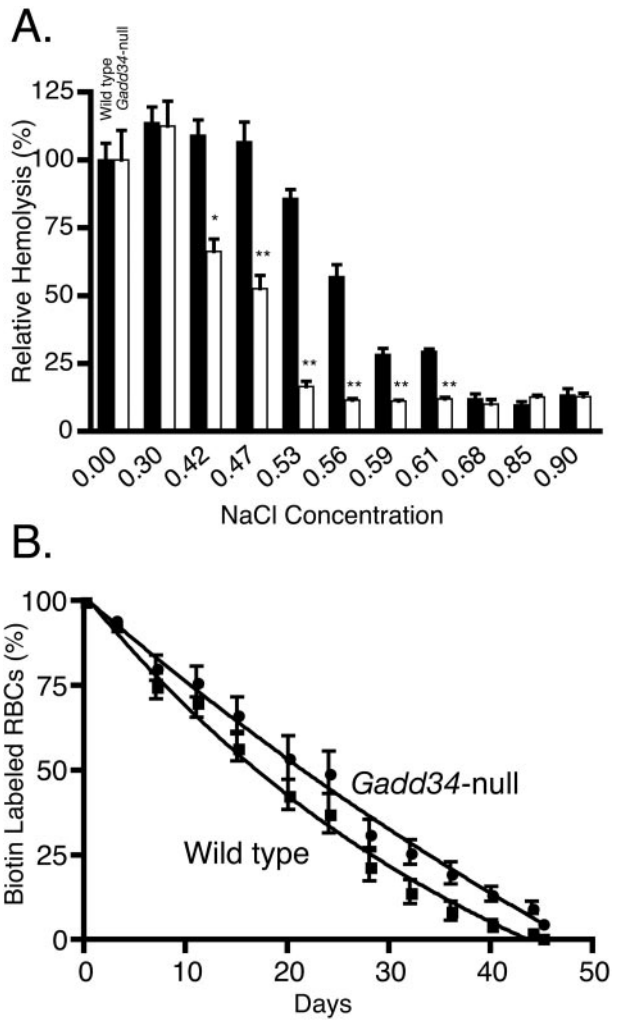

FIG. 4. *Gadd34*-null erythrocytes are more resistant to hemolysis under severe hypotonic conditions and have normal life spans. (A) Wild-type (black bars) and *Gadd34*-null (white bars) erythrocyte hemolysis in decreasing salt concentrations, as determined by absorbance of released hemoglobin at 540 nm. Data are plotted as means for three mice from each genotype normalized to complete lysis (0.0% NaCl) ± standard errors of the mean. *, $P < 0.05$; **, $P < 0.01$. (B) Erythrocyte (RBC) half-life was determined by measuring the disappearance of NHS-biotin from circulating erythrocytes. The wild-type erythrocyte half-life was 17 days, and the *Gadd34*-null erythrocyte half-life was 21.6 days ($P = 0.19$).

between groups, although it appears that *Gadd34*-null mice have increased expression of β_{minor}. Overall, globin chain synthesis is balanced in both genotypes, as demonstrated by comparison of the total β- to α-globin ratio.

Reticulocyte analyses. Expression of Gadd34 is typically induced during recovery from stress, such as that induced by thapsigargin. In terms of globin synthesis regulation, Gadd34 expression should be detectable in reticulocytes since PP1c requires Gadd34 targeting to exert its phosphatase activity on p-eIF2α(S51). In reticulocyte lysates from wild-type mice, Gadd34 protein was detected as a roughly 100-kDa band independent of the addition of 40 μM hemin (Fig. 6A).

Since Gadd34 functions in the recovery from protein synthesis attenuation following ER stress, we thought this stimulatory function on translation initiation might apply to other contexts, such as globin translation in reticulocytes where protein synthesis is very high. With the addition of hemin, the predominant eIF2α(S51) kinase in reticulocytes, HRI, becomes inactivated and protein synthesis initiation proceeds at an accelerated rate (2, 24). To monitor the effect of hemin addition on intact reticulocytes in wild-type and *Gadd34*-null mice, we enriched the blood cell population for reticulocytes with phenylhydrazine. Phenylhydrazine enrichment results in the peroxidation and ultimate hemolysis of mature erythrocytes, thus stimulating the production of reticulocytes in the bone marrow and ultimately their release into the bloodstream (12). After hemin addition, wild-type erythrocytes show a modest reduction in levels of p-eIF2α(S51), while the *Gadd34*-null reticulocytes maintain substantial and constitutive p-eIF2α(S51) levels (Fig. 6B). Also, the initial levels of p-eIF2α(S51) (time zero, Fig. 6B) were consistently higher in the *Gadd34*-null reticulocytes than in the wild-type reticulocytes.

Phosphorylation of eIF2α(S51) results in reduced formation of 43S preinitiation complexes, followed by runoff of the multiple, actively translating ribosomal complexes (polysomes)

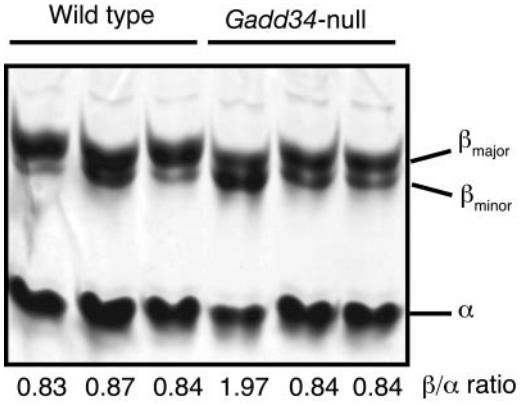

FIG. 5. *Gadd34*-null mice express normal globin chains. Hemoglobin from three wild-type and *Gadd34*-null mice was separated by TAU gel electrophoresis. β_{major}-, β_{minor}-, and α-globin are labeled at the right. The ratio of β- to α-globin is indicated at the bottom for each mouse.

and a general increase in mRNA bound to single ribosomes (monosomes, 40S, 60S, and 80S). Based on the levels of p-eIF2α(S51) in *Gadd34*-null reticulocytes, we were interested in profiling the polysomes of reticulocytes immediately after harvest from phenylhydrazine-treated mice (Fig. 6C). This method would be expected to provide a snapshot of the translation initiation machinery devoid of any additional stresses (e.g., incubation at 37°C). The wild-type reticulocytes (polysome to monosome ratio, 0.75 ± 0.15; $n = 6$) were consistently found to have a higher percentage of polysomes (Fig. 6C, top), and the *Gadd34*-null reticulocytes (polysome-to-monosome ratio, 0.50 ± 0.08; $n = 6$) were consistently found to have fewer polysomes ($P = 0.0057$) (Fig. 6C, bottom).

Iron-deficient diet. The phenotype of *Gadd34*-null mice is relatively mild without any apparent stress. However, if HRI kinase activity were increased due to iron deficiency, *Gadd34*-null mice would be expected to have a lower rate of recovery due to sustained p-eIF2α(S51). Failure to recover from iron deficiency would not be expected in the *Gadd34*-null mice, since the erythrocyte population is constantly being regenerated. Iron deficiency is characterized by marked reductions in MCV and MCH, as well as by erythrocyte hyperplasia. In general, the groups on the basal diet were mildly affected by the bimonthly bleeding schedule, as indicated by an increase in circulating red blood cells, a slight decrease in hemoglobin, and mildly reduced MCV and MCH levels. Following 8 weeks on the iron-deficient diet, wild-type mice recovered to near normal levels, as indicated by levels of MCV (recovered to 96.4% of the wild-type basal diet group) and MCH (recovered to 97.3% of the wild-type basal diet group) (Fig. 7, top). The *Gadd34*-null mice approached normal levels, as indicated by MCV (recovered to 91.3% of the *Gadd34*-null basal diet group) and MCH (recovered to 95.7% of the *Gadd34*-null basal diet group) (Fig. 7, bottom). Interestingly, the phase of erythrocyte hyperplasia in the *Gadd34*-null mice on the iron-deficient diet was delayed compared to the wild-type mice on

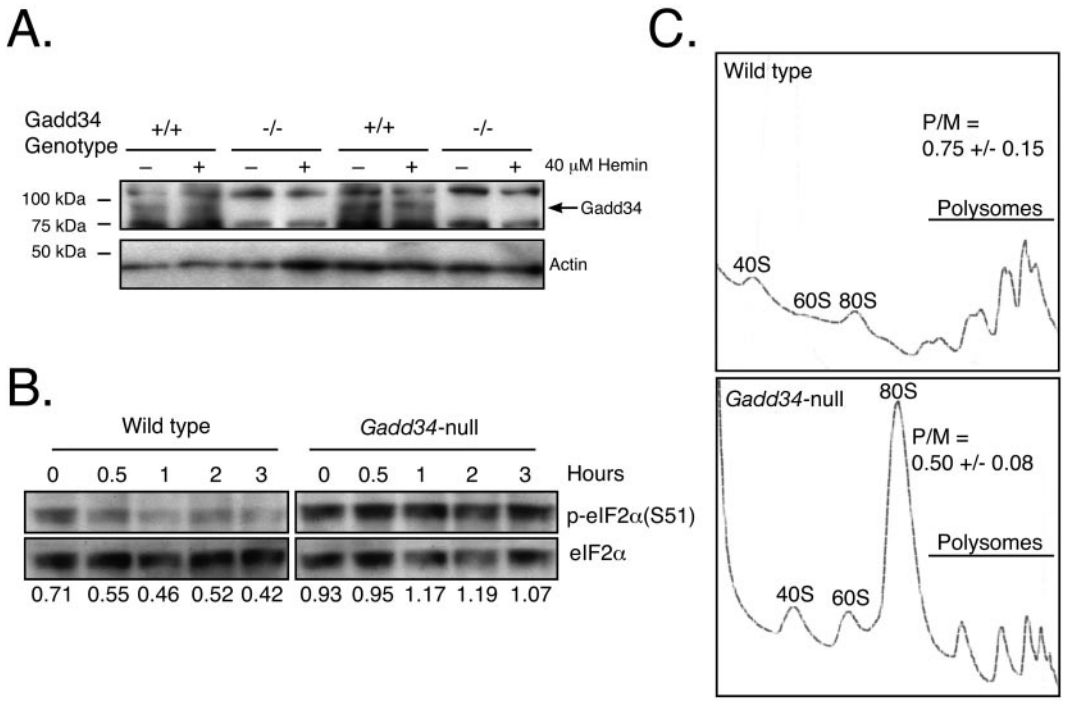

FIG. 6. *Gadd34*-null reticulocytes have attenuated translation initiation machinery. (A) Gadd34 expression was monitored after 3 hours of incubation with hemin. Actin is shown as a loading control. (B) Western blot of reticulocyte protein lysates following treatment with the hemoglobin synthesis activator hemin. Top, p-eIF2α(S51); bottom, total eIF2α. Densitometry was used to calculate the ratio of p-eIF2α (S51) to total eIF2α (indicated below each lane). (C) Polysome profiles from wild-type ($n = 6$) and *Gadd34*-null ($n = 6$) reticulocytes. Sixteen OD_{260} units were loaded for each sample, and polysome-to-monosome (P/M) ratios were determined by calculating the areas under the monosome and polysome peaks. Data are presented as averages ± standard errors of the mean.

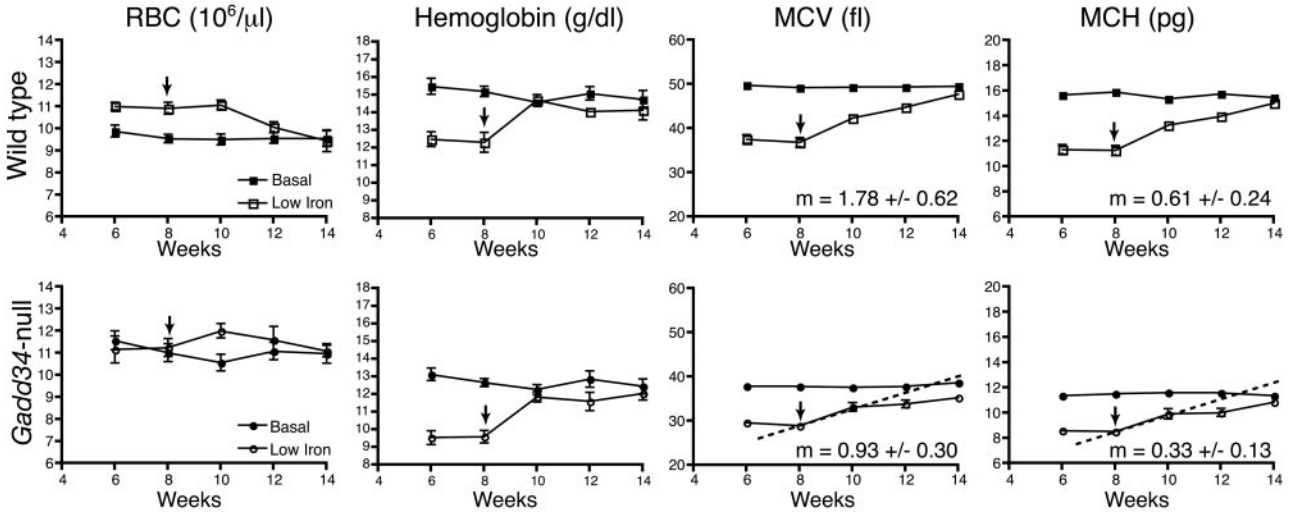

FIG. 7. *Gadd34*-null mice recover slowly from iron deficiency. Wild-type and *Gadd34*-null weanlings were placed on a basal or iron-deficient diet. Mice on the iron-deficient diet were returned to the basal diet after 8 weeks (designated by arrows). Slopes (m) for MCV and MCH were calculated from the best-fit line of values from weeks 8 through 14. Data for wild-type (basal diet, five males and two females; iron-deficient diet, six males and three females) and *Gadd34*-null (basal diet, three males and three females; iron-deficient diet, four males and four females) mice are presented as averages of all values for each genotype and parameter ± standard errors of the mean. *P* values were calculated by ANOVA. RBC, red blood cell.

the same diet. While both groups were able to recover, it was the overall rates of recovery that differed greatly between groups (MCV and MCH). The rate of recovery was determined by calculating the slope of the line formed from week 8 to week 14. The MCV slope for wild-type mice was 1.78 ± 0.62, and the slope for *Gadd34*-null mice was 0.93 ± 0.30 ($P = 0.003$). The MCH slope for wild-type mice was 0.61 ± 0.24, and the slope for *Gadd34*-null mice was 0.33 ± 0.13 ($P = 0.01$). In general, recovery from iron deficiency in wild-type mice was nearly twice as fast as that of *Gadd34*-null mice over a 6-week period.

DISCUSSION

This is the first report to identify a physiologic role for Gadd34, and we extend the protein synthesis recovery function of Gadd34 by demonstrating a novel role for Gadd34 in modulating hemoglobin synthesis. This evidence suggests that Gadd34 function is conserved across multiple signaling pathways involving eIF2α(S51) kinases.

Unstressed *Gadd34*-null mice exhibit a phenotype nearly opposite the unstressed phenotype of *HRI*-null mice. This is consistent with the opposing effects of HRI kinase and Gadd34/PP1c on eIF2α(S51) phosphorylation and globin synthesis in reticulocytes. *Gadd34*-null mice have reduced hemoglobin content (Table 1), while *HRI*-null mice have increased hemoglobin content (9). Observations with both *HRI*- and *Gadd34*-null mice support the finding that even in very low stress states both proteins are active and that a general equilibrium exists between kinase and phosphatase activities on eIF2α(S51) in order for the translation machinery to be properly regulated.

In wild-type reticulocytes, it is only during periods of more severe stress (e.g., iron deficiency or oxidative damage) that HRI kinase activity predominates and translation is repressed (9, 17). Translation can then be restored by the inactivation of HRI kinase by hemin, leading to eIF2α(S51) dephosphorylation and to resumption of normal steady-state activities of both kinase and phosphatase in the reticulocyte. Even with the addition of hemin to inactivate HRI kinase signaling, the *Gadd34*-null reticulocytes maintain high levels of translation initiation repression as a result of the inability to reverse the activity of HRI kinase (Fig. 6B). Increased levels of both p-eIF2α(S51) and monosomes suggest that the translation initiation machinery is repressed (Fig. 6B and C). In fact, the increase in monosome peaks is reminiscent of the polysome profiles of yeast eIF2B mutants that have reduced eIF2 activity (26). Furthermore, this suggests that both Gadd34 (in association with PP1c) and HRI kinase are necessary for the regulation of translation initiation in the mouse reticulocyte. The normal equilibrium existing between HRI kinase and Gadd34/PP1c can be shifted with the deletion of these genes in mice, favoring either the overproduction (in *HRI*-null mice) or underproduction (in *Gadd34*-null mice) of globin proteins.

The equilibrium between Gadd34 and HRI can also be shifted to favor highly active HRI kinase by iron deficiency. Iron deficiency is the most common nutritional deficiency in the world. Activation of HRI kinase in response to iron deficiency represents a key stress response to avoid the deleterious overproduction of globin in the reticulocyte. Recovery from translation initiation attenuation after a period of iron deficiency, much like the integrated stress response in the ER, appears to also require Gadd34 and subsequent targeting of PP1c to p-eIF2α(S51). The fact that the *Gadd34*-null mice are able to recover at all indicates that the overall pathway of erythropoiesis is functional. However, this does not rule out the possibility that other PP1c phosphatase complexes, such as constitutive repressor of eIF2α phosphorylation (CReP)/PP1c, can substitute for the lack of Gadd34, albeit less efficiently.

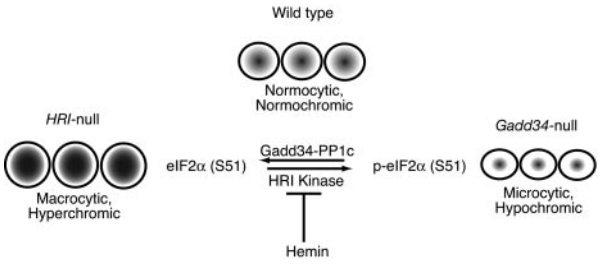

FIG. 8. Equilibrium between Gadd34/PP1c and HRI controls hemoglobin production. Abundant hemin prevents induction of HRI kinase activity above its basal role. Normocytic, normochromic erythrocytes arise from the balanced activities of Gadd34/PP1c and HRI kinase (center). Lack of HRI kinase (*HRI*-null) shifts the equilibrium toward unphosphorylated eIF2α(S51), favoring translation initiation and resulting in macrocytic, hyperchromic erythrocytes (left). Lack of Gadd34 (*Gadd34*-null), and hence failed recruitment of PP1c, shifts the equilibrium toward p-eIF2α(S51), favoring translation initiation attenuation and resulting in microcytic, hypochromic erythrocytes (right).

Since it appears that Gadd34/PP1c and HRI kinase directly oppose each other in the reticulocyte during hemoglobin synthesis, we propose a model in which Gadd34/PP1c and HRI kinase exist in an equilibrium state (Fig. 8). In the wild-type setting, active translation initiation is favored by the inhibition of HRI kinase in a plentiful heme environment (Fig. 8, center), producing normocytic, normochromic mature red blood cells. When HRI kinase is removed, overactive translation initiation is favored (Gadd34/PP1c activity is predominant), resulting in hyperchromic, macrocytic red blood cells (Fig. 8, left). When Gadd34 is removed from the equilibrium, maintenance of translation initiation attenuation is favored (HRI kinase activity is predominant), resulting in hypochromic, microcytic red blood cells (Fig. 8, right).

Currently, thalassemias have mostly been associated with the mutation of globin genes, resulting in decreased expression of the α- or β-globin chains. However, roughly 10% of the thalassemias are determined to have normal globin genes, with disease possibly resulting from defects in the actual transcription or translational machinery (7, 8). Our proposal that improper translation of globin mRNA can result in a thalassemia-like phenotype is supported by the fact that *Gadd34*-null mice can produce normal hemoglobin tetramers yet cannot produce hemoglobin in amounts comparable to their wild-type counterparts (Fig. 5; Table 1). In addition to the decreased hemoglobin in the erythrocytes, the *Gadd34*-null phenotype is also consistent with a thalassemia-like condition, as these mice have hypersplenism, increased resistance to hemolysis in hypotonic solutions, and expanded populations of immature erythroid precursors in the spleen (Fig. 2A to C). The spleen abnormalities are most likely associated with extramedullary hematopoiesis due to insufficient hemoglobin concentration in the circulating erythrocyte population. Extensive searches of online databases for known thalassemias have not revealed any thalassemia disease loci in close proximity to the *Gadd34* gene, yet this does not completely rule out the possibility that Gadd34 or HRI might be linked to these diseases.

The concept of Gadd34 as a translation initiation regulator is not new; however, the engineering of *Gadd34*-null mice has allowed us to characterize a novel physiologic role for Gadd34 during erythrocyte development. Furthermore, since the phenotype of *HRI*-null mice is nearly opposite the phenotype of *Gadd34*-null mice, these findings represent an important regulatory role for Gadd34/PP1c and HRI kinase in translation initiation regulation of mouse reticulocytes.

REFERENCES

1. **Alter, B. P., S. C. Goff, G. D. Efremov, M. E. Gravely, and T. H. Huisman.** 1980. Globin chain electrophoresis: a new approach to the determination of the G gamma/A gamma ratio in fetal haemoglobin and to studies of globin synthesis. Br. J. Haematol. **44:**527–534.
2. **Bauer, B. N., M. Rafie-Kolpin, L. Lu, A. Han, and J. J. Chen.** 2001. Multiple autophosphorylation is essential for the formation of the active and stable homodimer of heme-regulated eIF2alpha kinase. Biochemistry **40:**11543–11551.
3. **Brush, M. H., D. C. Weiser, and S. Shenolikar.** 2003. Growth arrest and DNA damage-inducible protein GADD34 targets protein phosphatase 1α to the endoplasmic reticulum and promotes dephosphorylation of the α subunit of eukaryotic translation initiation factor 2. Mol. Cell. Biol. **23:**1292–1303.
4. **Chefalo, P. J., J. Oh, M. Rafie-Kolpin, B. Kan, and J. J. Chen.** 1998. Heme-regulated eIF-2alpha kinase purifies as a hemoprotein. Eur. J. Biochem. **258:**820–830.
5. **Chomczynski, P., and N. Sacchi.** 1987. Single-step method of RNA isolation by acid guanidinium thiocyanate-phenol-chloroform extraction. Anal. Biochem. **162:**156–159.
6. **Connor, J. H., D. C. Weiser, S. Li, J. M. Hallenbeck, and S. Shenolikar.** 2001. Growth arrest and DNA damage-inducible protein GADD34 assembles a novel signaling complex containing protein phosphatase 1 and inhibitor 1. Mol. Cell. Biol. **21:**6841–6850.
7. **Gibbons, R. J., D. J. Picketts, L. Villard, and D. R. Higgs.** 1995. Mutations in a putative global transcriptional regulator cause X-linked mental retardation with alpha-thalassemia (ATR-X syndrome). Cell **80:**837–845.
8. **Gu, X., and Y. Zeng.** 2002. A review of the molecular diagnosis of thalassemia. Hematology **7:**203–209.
9. **Han, A. P., C. Yu, L. Lu, Y. Fujiwara, C. Browne, G. Chin, M. Fleming, P. Leboulch, S. H. Orkin, and J. J. Chen.** 2001. Heme-regulated eIF2alpha kinase (HRI) is required for translational regulation and survival of erythroid precursors in iron deficiency. EMBO J. **20:**6909–6918.
10. **Harding, H. P., H. Zeng, Y. Zhang, R. Jungries, P. Chung, H. Plesken, D. D. Sabatini, and D. Ron.** 2001. Diabetes mellitus and exocrine pancreatic dysfunction in perk$^{-/-}$ mice reveals a role for translational control in secretory cell survival. Mol. Cell **7:**1153–1163.
11. **He, B., M. Gross, and B. Roizman.** 1997. The gamma(1)34.5 protein of herpes simplex virus 1 complexes with protein phosphatase 1alpha to dephosphorylate the alpha subunit of the eukaryotic translation initiation factor 2 and preclude the shutoff of protein synthesis by double-stranded RNA-activated protein kinase. Proc. Natl. Acad. Sci. USA **94:**843–848.
12. **Itano, H. A., K. Hirota, and K. Hosokawa.** 1975. Mechanism of induction of haemolytic anaemia by phenylhydrazine. Nature **256:**665–667.
13. **Kojima, E., A. Takeuchi, M. Haneda, A. Yagi, T. Hasegawa, K. Yamaki, K. Takeda, S. Akira, K. Shimokata, and K. Isobe.** 2003. The function of GADD34 is a recovery from a shutoff of protein synthesis induced by ER stress: elucidation by GADD34-deficient mice. FASEB J. **17:**1573–1575.
14. **Krishnamoorthy, T., G. D. Pavitt, F. Zhang, T. E. Dever, and A. G. Hinnebusch.** 2001. Tight binding of the phosphorylated α subunit of initiation factor 2 (eIF2α) to the regulatory subunits of guanine nucleotide exchange factor eIF2B is required for inhibition of translation initiation. Mol. Cell. Biol. **21:**5018–5030.
15. **Lakso, M., J. G. Pichel, J. R. Gorman, B. Sauer, Y. Okamoto, E. Lee, F. W. Alt, and H. Westphal.** 1996. Efficient in vivo manipulation of mouse genomic sequences at the zygote stage. Proc. Natl. Acad. Sci. USA **93:**5860–5865.
16. **Liebermann, D. A., and B. Hoffman.** 2003. Myeloid differentiation (MyD) primary response genes in hematopoiesis. Blood Cells Mol. Dis. **31:**213–228.
17. **Lu, L., A. P. Han, and J. J. Chen.** 2001. Translation initiation control by heme-regulated eukaryotic initiation factor 2α kinase in erythroid cells under cytoplasmic stresses. Mol. Cell. Biol. **21:**7971–7980.
18. **Ma, Y., and L. M. Hendershot.** 2003. Delineation of a negative feedback regulatory loop that controls protein translation during endoplasmic reticulum stress. J. Biol. Chem. **278:**34864–34873.
19. **Novoa, I., H. Zeng, H. P. Harding, and D. Ron.** 2001. Feedback inhibition of the unfolded protein response by GADD34-mediated dephosphorylation of eIF2alpha. J. Cell Biol. **153:**1011–1022.
20. **Novoa, I., Y. Zhang, H. Zeng, R. Jungreis, H. P. Harding, and D. Ron.** 2003. Stress-induced gene expression requires programmed recovery from translational repression. EMBO J. **22:**1180–1187.
21. **Paszty, C., N. Mohandas, M. E. Stevens, J. F. Loring, S. A. Liebhaber, C. M. Brion, and E. M. Rubin.** 1995. Lethal alpha-thalassaemia created by gene targeting in mice and its genetic rescue. Nat. Genet. **11:**33–39.

22. **Pestova, T. V., V. G. Kolupaeva, I. B. Lomakin, E. V. Pilipenko, I. N. Shatsky, V. I. Agol, and C. U. Hellen.** 2001. Molecular mechanisms of translation initiation in eukaryotes. Proc. Natl. Acad. Sci. USA **98:**7029–7036.
23. **Proud, C. G.** 2005. eIF2 and the control of cell physiology. Semin. Cell Dev. Biol. **16:**3–12.
24. **Rafie-Kolpin, M., P. J. Chefalo, Z. Hussain, J. Hahn, S. Uma, R. L. Matts, and J. J. Chen.** 2000. Two heme-binding domains of heme-regulated eukaryotic initiation factor-2alpha kinase. N terminus and kinase insertion. J. Biol. Chem. **275:**5171–5178.
25. **Rafie-Kolpin, M., A. P. Han, and J. J. Chen.** 2003. Autophosphorylation of threonine 485 in the activation loop is essential for attaining eIF2alpha kinase activity of HRI. Biochemistry **42:**6536–6544.
26. **Richardson, J. P., S. S. Mohammad, and G. D. Pavitt.** 2004. Mutations causing childhood ataxia with central nervous system hypomyelination reduce eukaryotic initiation factor 2B complex formation and activity. Mol. Cell. Biol. **24:**2352–2363.
27. **Socolovsky, M., H. Nam, M. D. Fleming, V. H. Haase, C. Brugnara, and H. F. Lodish.** 2001. Ineffective erythropoiesis in Stat5a(−/−)5b(−/−) mice due to decreased survival of early erythroblasts. Blood **98:**3261–3273.
28. **Srivastava, S. P., K. U. Kumar, and R. J. Kaufman.** 1998. Phosphorylation of eukaryotic translation initiation factor 2 mediates apoptosis in response to activation of the double-stranded RNA-dependent protein kinase. J. Biol. Chem. **273:**2416–2423.
29. **Vattem, K. M., and R. C. Wek.** 2004. Reinitiation involving upstream ORFs regulates ATF4 mRNA translation in mammalian cells. Proc. Natl. Acad. Sci. USA **101:**11269–11274.
30. **Whitney, J. B. R., A. Leder, J. Lewis, R. A. Popp, C. Paszty, E. M. Rubin, W. R. Shehee, T. M. Townes, and O. Smithies.** 1998. Rapid genotyping of mice with hemoglobinopathies and globin transgenes. Biochem. Genet. **36:**65–77.
31. **Wilkinson, K., J. Fikes, and S. Wojcik.** 2001. Improved mouse blood smears using the DiffSpin slide spinner. Vet. Clin. Pathol. **30:**197–200.
32. **Xu, X., C. Li, L. Garrett-Beal, D. Larson, A. Wynshaw-Boris, and C. X. Deng.** 2001. Direct removal in the mouse of a floxed neo gene from a three-loxP conditional knockout allele by two novel approaches. Genesis **30:**1–6.
33. **Zhang, P., B. C. McGrath, J. Reinert, D. S. Olsen, L. Lei, S. Gill, S. A. Wek, K. M. Vattem, R. C. Wek, S. R. Kimball, L. S. Jefferson, and D. R. Cavener.** 2002. The GCN2 eIF2α kinase is required for adaptation to amino acid deprivation in mice. Mol. Cell. Biol. **22:**6681–6688.